

Study on moisture transport in concrete in atmospheric environment

Weiping Zhang^{*}, Fei Tong^a, Xianglin Gu^b and Yunping Xi^c

Department of Structural Engineering, Tongji University, 1239 Siping Road, Shanghai 200092, China

(Received March 2, 2015, Revised October 31, 2015, Accepted November 12, 2015)

Abstract. Moisture transport in concrete in atmospheric environment was studied in this paper. Based on the simplified formula of the thickness of the adsorbed layer, the pore-size distribution function of cement paste was calculated utilizing the water adsorption isotherms. Taking into consideration of the hysteresis effect in cement paste, the moisture diffusivity of cement paste was obtained by the integration of the pore-size distribution. Concrete is regarded as a two-phase composite with cement paste and aggregate, neglecting the moisture diffusivity of aggregate, then moisture diffusivity of concrete was evaluated using the composite theory. Finally, numerical simulation of humidity response during both wetting and drying process was carried out by the finite difference method of partial differential equation for moisture transport, and the numerical results well capture the trend of the measured data.

Keywords: concrete; moisture transport; atmospheric environment; pore-size distribution

1. Introduction

Moisture transport in concrete is an important factor affecting the durability of concrete. Corrosive ions in the ambient environment, such as chloride ion and sulfate ion, can penetrate into concrete only after being dissolved into pore water in concrete. For reinforced concrete structures in the atmospheric environment, water also plays an important role in the reaction process of carbonation and reinforcement corrosion. Different boundary conditions represent different wetting process and mechanism. When the outside of concrete is full of liquid water, the process of liquid water moving into the unsaturated concrete under ambient pressure or capillary pressure can be called as water absorption. While if the concrete is in atmospheric environment with a high humidity, the ingress of vapor in air into the concrete should be recognized as moisture adsorption.

Through assuming the relationship between the moisture diffusivity and relative humidity/water content and data fitting of experimental data, many empirical models for moisture diffusivity have been proposed by researchers, such as Bažant and Najjar (1972), Sakata (1983),

^{*}Corresponding author, Professor, E-mail: weiping_zh@tongji.edu.cn

^aMaster Student, E-mail: tongfei_1990@126.com

^bProfessor, E-mail: gxl@tongji.edu.cn

^cProfessor, E-mail: yunping.xi@colorado.edu

Xi *et al.* (1994a), Garrabrants and Kosson (2003), Leech *et al.* (2003). In the experiments of moisture transport in concrete, concrete specimens were initially wet and then exposed to a lower constant environmental humidity except for the ones in Leech *et al.* (2003), which were initially dried and then contacted with liquid water. For the different wetting or drying process of concrete, there might be considerable difference in magnitude between different tested results of moisture diffusivity Daian (1988), Li (2010). And empirical models usually describe the moisture transport in a macroscopic and apparent way, without direct relation to mechanism of moisture transport in concrete. In that case, numerous researchers got their transport models in theoretical way by the application of classical transport theory, or composite material theory. To consider the influence of saturation degree and microstructural characteristics, both Zhang (2012) and Li (2009) introduced relative permeability of liquid water k_{lr} and hindrance diffusion coefficient of water vapor $f(S, \Phi)$, which are empirical coefficients, into macroscopic transport equations, leading to the limitation of their models. Maekawa *et al.* (2009), Ishida *et al.* (2007), Guo (2013) obtained diffusivities by the integration of the pore-size distribution. Inner transport mechanism were embodied in the models, however, pore-size distributions of concrete in their models were approximated by a simplistic Raleigh-Ritz distribution function or measured values by mercury intrusion porosimetry (MIP).

In fact, there are discrepancies in pore characteristics between cement paste and aggregate, which are two constituent parts of concrete Hall and Hoff (2012), Winkler (1994), Siegesmund (2011). And the discrepancies should be taken consideration into the moisture diffusivity models. Concrete is commonly regarded as a composite of cement paste (continuous phase) and aggregate (discontinuous phase), and the diffusivity can be obtained by the composite theory, such as Ababneh *et al.* (2003) and Eskandari-Ghadi *et al.* (2013). However, diffusivity of each phase in their models is still empirical.

Concrete is a kind of complex porous media. Only with pore inside, ambient moisture may have access to the inside and move within, and the diffusivity is closely related to the internal pore characteristics. So model for diffusivity of moisture transport can be theoretically feasible once they are expressed in terms of pore characteristics. A calculation procedure to predict the humidity distribution was demonstrated in this paper. Pore-size distribution and moisture diffusivity of cement paste is obtained by using adsorption isotherm. Moisture diffusivity of concrete is calculated by composite theory, and then humidity response in cement paste or concrete can be predicted.

2. Moisture transport in concrete

2.1 Partial differential equations for moisture transport

Water movement in the pore during the wetting process of a porous material, which are originally dry, can be described as the following stages Rose (1963): (a) Gaseous water molecules, subjecting to the strong adsorption of pore wall, enter the pore by adsorption and surface diffusion and form the adsorption water layer gradually. (b) When the layer becomes thicker and thicker, the adsorption of the pore wall will be weakened, and the unimpeded transport of water vapor can be described by diffusion equation. (c) As the internal humidity in the pore increases, capillary condensation happens and the adsorbed layer forms a meniscus (liquid islands) at the neck, i.e., a narrow connection between larger pores, and water vapor condensates at one side and liquid evaporates on the other side, shortening the effective path length for diffusion of vapor and

accelerating the vapor transport. (d) When the internal relative humidity comes to a critical point, condensation water fills the pores and becomes hydraulic flow. It can be seen that the predominant transport mechanism will transfer from vapor diffusion to liquid flow as the wetting process proceed, which have already be found in the experiments Daian (1988).

It has been found that total water content W of concrete will change during the hydration of cement, while relative humidity h almost remains the same Bažant and Najjar (1972), Xi *et al.* (1994b). And also, for concrete in atmospheric environment, the boundary conditions are given as humidity h instead of W . So term $grad(h)$ is used other than $grad(W)$ to describe the moisture flux J at isothermal condition, that is

$$J = -D_h grad(h) \quad (1)$$

which can be rewritten according to the mass conservation

$$\rho_d \frac{\partial W}{\partial t} = \rho_d \frac{\partial W}{\partial h} \frac{\partial h}{\partial t} = -div(J) = div(D_h grad(h)) \quad (2)$$

Where W is total water content, kg/kg; $\partial W/\partial h$ is moisture capacity, derivative of the relationship between W and h (that is adsorption isotherms), ρ_d is apparent density for dry materials, kg/m³; D_h is moisture diffusivity, kg/(m•s), reflecting the velocity of internal moisture transport in cementitious materials and varying with the internal relativity humidity.

2.2 Equilibrium water condensation

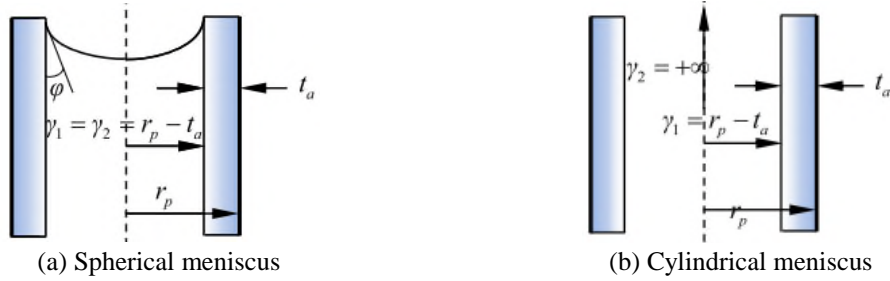
Both condensation and decondensation occurs in the pore during the moisture transport. As moisture moves slowly, and the exchange rate on the vapor-liquid interface is very large, so that the equilibrium at the interface can be reached instantaneously and local thermodynamic equilibrium be assumed Rose (1963), Daian (1989). Due to the discontinuity of the inner pressure on the vapor-liquid interface in unsaturated materials, capillary pressure generates and drives the movement of liquid water. Based on the thermodynamic equilibrium theory, Kelvin's equation gives the equilibrium relationship between equilibrium relative humidity and capillary pressure Daian (1988)

$$\ln h_k = \frac{p_c M_w}{\rho_l RT} \quad (3)$$

where h_k is equilibrium relative humidity, which is required to fully saturate the pore; p_c is capillary pressure, Pa; M_w is molar mass of water, 0.018kg/mol; ρ_l is liquid water density, 1000kg/m³; R is gas constant, 8.3144J/(mol•K), and T is thermodynamic temperature, K.

In fact, the pressure difference between the liquid and vapor phases would be balanced by the curved vapor-liquid interface formed in numerous pores of the microstructure. And the Young-Laplace's equation presents the relationship between curvature radius and capillary pressure Zhang (2012), Gawin *et al.* (1999).

$$p_c = -\sigma \left(\frac{1}{\gamma_1} + \frac{1}{\gamma_2} \right) = -\frac{\sigma}{R_c} \quad (4)$$

Fig. 1 The relationship between r_p and r_k

Where γ_1, γ_2 are curvature radii in different directions respectively, m; $1/R_c$ is the sum of reciprocal of γ_1 and γ_2 , m; σ is surface tension and 0.07219N/m at 20°C.

When capillary condensation occurs, the interface was commonly assumed as spherical (Fig. 1(a)) with $\gamma_1 = \gamma_2 = (r_p - t_a) / \cos\varphi$, where φ is contact angle between meniscus and pore wall. Because the pore wall is rough, φ can be very small, $\cos\varphi$ can be taken to be 1 for common case (Zhang 2012). Then Eq. (4) turns to

$$R_c = \frac{1}{\cos\varphi/(r_p - t_a) + \cos\varphi/(r_p - t_a)} = \frac{r_p - t_a}{2} = \frac{r_k}{2} \quad (5)$$

Where r_p is actual radius, m; t_a is thickness of adsorbed layer on pore wall, m; r_k is equilibrium radius (also can be called Kelvin radius) maintaining the meniscus, which is smaller than the actual radius and equals to $r_p - t_a$.

When only adsorption water exists, the interface was assumed as cylindrical. Then $\gamma_1 = (r_p - t_a)$, $\gamma_2 = +\infty$ (Fig. 1(b)) and R_c becomes

$$R_c = \frac{1}{1/(r_p - t_a) + 1/+\infty} = r_p - t_a = r_k \quad (6)$$

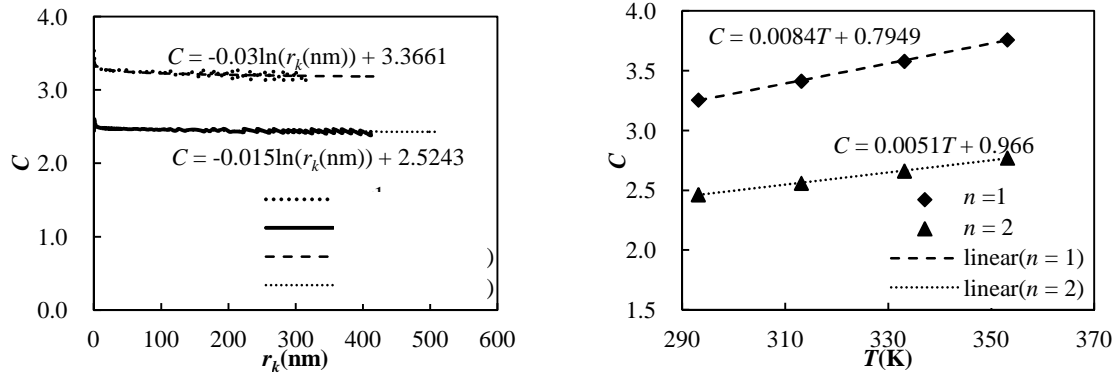
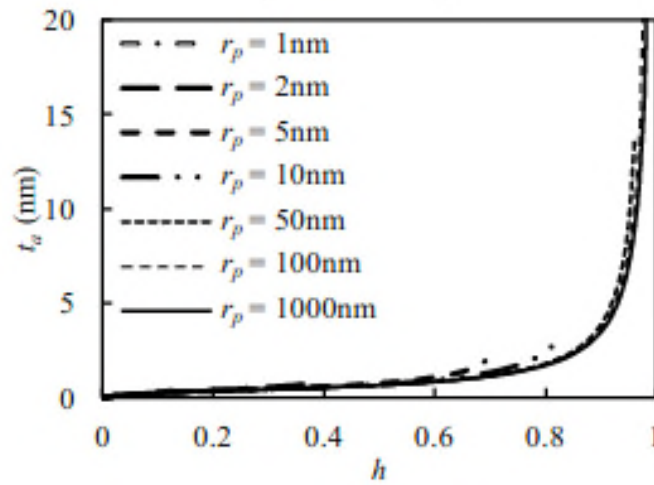
Combine the equations from Eq. (3) to Eq. (6), Kelvin's Equation can be converted into

$$h_k = \exp\left(-\frac{n\sigma M_w}{\rho_l RT r_k}\right), \quad \text{where } \begin{cases} n=1, & \text{Cylindrical meniscus} \\ n=2, & \text{Spherical meniscus} \end{cases} \quad (7)$$

2.3 Thickness of adsorbed layer

Different from the liquid water in the natural state, adsorbed layer, subjected to the strong Van der Waal's force of the pore wall, is condensed in the medium and hard to move. A modified statistical formula for thickness of adsorbed layer was proposed by Hillerborg (1985), accounting for the pore shape and surface tension (m)

$$t_a(h) = \frac{5.25h \times 10^{-9}}{(1 - h/h_k)(1 - h/h_k + 15h)} \quad (8)$$

Fig. 2 Relationship between C and r_k , T Fig. 3 t_a values for pores without condensation ($T=273.15\text{K}$)

Where t_a is thickness of adsorbed layer, m. Due to Eq. (8) is implicit in t_a , some iterative scheme must be used to generate the thickness of every pore in each step in the latter numerical analysis. Clearly, it would be a time-consuming task and pose practical limitations, so some simplification work is needed.

Define parameter $C = r_p/r_k$, then $t_a(h_k) = (C-1)r_k$. Taking both $t_a(h_k) = (C-1)r_k$ and Eq. (7) into Eq. (8), the relationship between C and r_k or T was obtained separately by numerous calculations at the range of 1-1000nm of r_p , as shown in Fig. 2. Then the simplified formula for C can be regressed as

$$C = \begin{cases} -0.03\ln(r_k \times 10^9) + 0.0084T + 0.9052, & n = 1 \\ -0.15\ln(r_k \times 10^9) + 0.0051T + 1.0258, & n = 2 \end{cases} \quad (9)$$

For the pores without condensation, thicknesses of the adsorbed layer for pores with different

Table 1 Cement type in ASTM and values for V_{ct} and N_{ct}

ASTM Type	ASTM Designation	Composition				Fineness (cm ² /g)	Compressive strength % of type I cement*			V_{ct}	N_{ct}
		C ₃ S	C ₂ S	C ₃ A	C ₄ AF		1d	2d	28d		
I	General purpose	50	24	11	8	1800	100	100	100	0.9	1.1
II	Moderate sulfate resistant Moderate Heat of hydration	42	33	5	13	1800	75	85	90	1	1
III	High early strength	60	13	9	8	2600	190	120	110	0.85	1.15
IV	Low heat	26	50	5	12	1900	55	55	75	0.6	1.5
V	Sulfate resisting	40	40	4	9	1900	65	75	85	/	/

*All cements attain almost the same strength at 90 days.

radius were calculated, and the results were shown in Fig. 3. It can be seen from the figure that, t_a of pores with different sizes is almost the same under the same humidity. In order to simplify the later numerical calculation, t_a for pores without condensation were replaced by the ones of the smallest pores, which only have adsorbed layers on the pore wall.

3. Adsorption and desorption isotherms

3.1 Adsorption isotherms

Adsorption isotherm reflects the equilibrium relationship between water content and humidity during adsorption process. Proposed by Brunauer *et al.* (1938) and later developed by Brunauer *et al.* (1969), the modified three-parameter BET models (BSB model) is commonly used to describe adsorption in porous media. A semi-empirical mathematical model for adsorption isotherm of cementitious materials was proposed by Xi *et al.* (1994b). Based on the available adsorption test data, some empirical formulas for these parameters in the model were established by taking into consideration of the original water cement ratio, curing time, temperature and cement type. Water adsorbed in the pores with the relative humidity of h in kilograms of water per kilogram of cement paste (kg/kg) W_{cp} can be obtained by the following formula, where V_m is monolayer capacity in kilograms per kilogram of cement paste, kg/kg; C_T is constant related to temperature and heat of adsorption; n_l is the number of layers when $h=1$ in cement paste and k is related to n_l ; w/c is water cement ratio, for $w/c \leq 0.3$ set 0.3, for $w/c \geq 0.7$ set 0.7; t is curing time, for $t \leq 5d$ set 5d; V_{ct} and N_{ct} reflect the influence of different cement types to V_m and n_l respectively, and values for V_{ct} and N_{ct} given by Xi *et al.* (1994b) for different types of cement (ASTM C150), Ramachandran and Feldman (1984) were listed in Table 1. Values of V_{ct} and N_{ct} for cement type I were used in the following numerical calculations.

$$W_{cp} = \frac{C_T k V_m h}{(1 - kh) [1 + (C_T - 1) kh]} \quad (10)$$

$$\begin{cases} V_m = \left(0.068 - \frac{0.22}{t}\right) \left(0.85 + 0.45 \frac{w}{c}\right) V_{ct} \\ C_T = \exp\left(\frac{855}{T}\right) \\ k = \left[1 - \frac{1}{n_l} C_T - 1\right] / (C_T - 1) \\ n_l = \left(2.5 + \frac{15}{t}\right) \left(0.33 + 2.2 \frac{w}{c}\right) N_{ct} \end{cases} \quad (11)$$

Moisture capacity of cement paste $\partial W_{cp} / \partial h$ is the derivative of the Eq. (10) and

$$\frac{\partial W_{cp}}{\partial h} = \frac{C_T k V_m + W_{cp} k [1 + (C_T - 1)kh] - W_{cp} k (1 - kh)(C_T - 1)}{(1 - kh)[1 + (C_T - 1)kh]} \quad (12)$$

3.2 Pore-size distribution function calculated with adsorption isotherms

Pore-size distribution function $G(r)$ represents the fractional pore volume of the distribution for pore with radius r , which describes the probability of r in (r_{\min}, r_{\max}) . Assuming that all the pores are of the same length, the distribution probabilities, which are isotropy, are proportional to their respective cross section area on each cross section of the porous material. The following equation should be satisfied

$$\int_{r_{\min}}^{r_{\max}} G(r) dr = 1 \quad (13)$$

Since the correlations between moisture content and relative humidity are dependent on $G(r)$, $G(r)$ can be obtained by the adsorption or desorption isotherm. Barrett *et al.* (1951) came up with the BJH method for estimating the volume and area of pores utilizing desorption isotherm. Considering the lack of models of desorption isotherm for cementitious materials and existence of hysteresis effect, which holds the probability of saturation for pores with the radius bigger than equilibrium radius, the BJH method was modified by Cranston and Inkley CI method (1957). In spite of the usage of adsorption isotherm in CI method other than desorption isotherm, both CI and BJH method can be referred to as BJH method in nature owing to their similar principle: when there is an increment of relative humidity Δh inner the material, condensation in some pores happens in some pores, while adsorption layer thickens in others, and the increment of total moisture content ΔW is the sum of both.

Cylindrical-shaped pores were assumed in this paper. Given the actual radius, equilibrium radius, equilibrium humidity and total length per unit mass are r_{pi} , r_{ki} , h_{ki} and L_i for pore i respectively, so the volume of pore i per unit mass would be $V_{pi} = \pi r_{pi}^2 L_i$. Take $V_r(r)$ as the volume distribution for pore with radius r per unit mass, then $V_{pi} = \int V_r(r_{pi}) dr$.

When relative humidity increases from $h_{k,j-1}$ to $h_{kj} = h_{k,j-1} + \Delta h_j$, condensation happens in pore j , which represents the pore with radius from $r_{p,j-1}$ to $r_{pj} = r_{p,j-1} + \Delta r_j$, and the core radius for condensation being perpendicular to the axial direction changes from γ_{j-1} to γ_j , so does the equilibrium radius for corresponding pores from $r_{k,j-1} = 2\gamma_{j-1}$ to $r_{kj} = 2\gamma_j$. For the pores with radius bigger than r_{pj} (pores from j to $j+1$) meanwhile, thickness of adsorption layer increases from $t_{a,j-1}$

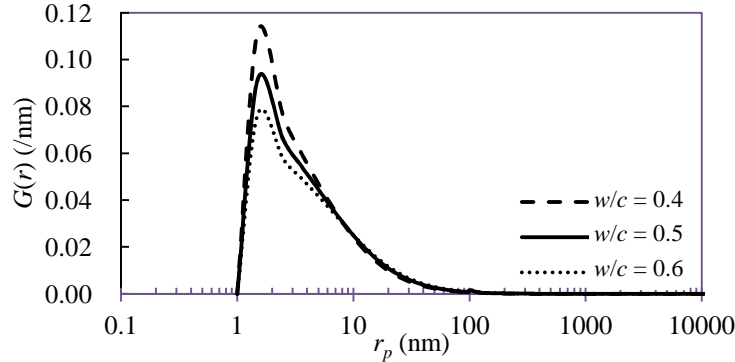


Fig. 4 $G(r)$ for hardened Portland cement paste with different water cement ratios

to $t_{aj} = t_{a,j-1} + \Delta t_{aj}$. Due to the small change of Δt_{aj} , the mean value $\bar{t}_{aj} = (t_{a,j-1} + t_{aj})/2$ was taken to represent the thickness of adsorption layer for radius range $(r_{p,j+1}, r_{\max})$ during the increment of relative humidity Δh_j . The total change of moisture volume ΔV_j caused by Δh_j can be established

$$\Delta V_j = \int_{r_{p0}}^{r_{pj}} \pi L_i (r_i - t_{a,j-1})^2 dr + (t_{aj} - t_{a,j-1}) \int_{r_{pj}}^{r_{\max}} 2\pi L_i (r_i - \bar{t}_{aj}) dr \quad (14)$$

Substitute $\bar{V}_{pi} = V_r(r_i)dr = \pi r_i^2 L_i$ into Eq. (14), and rewrite the integration form of second term right-hand yields

$$\Delta V_j = \frac{\bar{V}_{pj}}{\Delta r_j} \int_{r_{p,j-1}}^{r_{pj}} \frac{(r - t_{a,j-1})^2}{r^2} dr + 2\Delta t_{aj} \sum_{i=j+1}^n \frac{\bar{V}_{pi}}{\Delta r_i} \int_{r_{p,i-1}}^{r_{pi}} \frac{r - \bar{t}_{aj}}{r^2} dr \quad (15)$$

and

$$\frac{1}{\Delta r_j} \int_{r_{p,j-1}}^{r_{pj}} \frac{(r - t_{a,j-1})^2}{r^2} dr = 1 - 2 \frac{t_{a,j-1}}{\Delta r_j} \ln \frac{r_{pj}}{r_{p,j-1}} + \frac{t_{a,j-1}^2}{\Delta r_j} \left(\frac{1}{r_{p,j-1}} - \frac{1}{r_{pj}} \right) \quad (16)$$

$$\frac{1}{\Delta r_i} \int_{r_{p,i-1}}^{r_{pi}} \frac{r - \bar{t}_{aj}}{r^2} dr = \frac{1}{\Delta r_i} \left(\ln \left(\frac{r_{pi}}{r_{p,i-1}} \right) + \bar{t}_{aj} \left(\frac{1}{r_{pi}} - \frac{1}{r_{p,i-1}} \right) \right) \quad (17)$$

With the given adsorption isotherm $W-h$ of dry cement paste, relationship between ΔW_j and Δh_j can be calculated, so does the ΔV_j (dividing ΔW_j by liquid water density ρ_l) and Δh_j . Calculating with the three above equations, and starting at the biggest humidity h_n , pore volumes $\bar{V}_{pn}, \bar{V}_{p,n-1}, \dots, \bar{V}_{p,j}, \dots, \bar{V}_{p,2}$ and $\bar{V}_{p,1}$ can be obtained step by step, and the computed \bar{V}_{pj} should satisfy

$$\Phi = \rho_{cpd} \sum_{j=1}^{j=n} \bar{V}_{pj} \quad (18)$$

where ρ_{cpd} is apparent density for dry cement paste, kg/m³. Φ is porosity, m³/m³.

Pore-size distribution function $G(r)$ can be expressed as

$$G(r_{pj}) = V_r(r_{pj}) \rho_{cpd} = \frac{\overline{V}_{pj}}{\Delta r_j} \rho_{cpd} \quad (19)$$

where $G(r_{pj})$ represents the volume fraction for pore with the radius of r_{pj} in total volume, 1/m. Setting 0.4, 0.5 and 0.6 for water cement ratio in the adsorption model proposed by Xi *et al.* (1994b) respectively, computed results for $G(r)$ of hardened cement pasted of type I with 28 days of curing and 20°C were shown in Fig. 4. A key point here is that, for the micropores with radius closed to molecular size, the adsorption potential is so large that the condensed liquid water in micropores are distinct from the nature capillary condensation in bigger pores, leading to inapplicability of Kelvin's equation Kondo *et al.* (2005), so the pores with the radius smaller than 1nm was omitted during the calculation. All of the $G(r)$ in Fig. 4 are distributions with sole peak around 2nm, which decreases with the increase of water cement ratio, and also the width for $G(r)$ before the $r_p = 10\text{nm}$ have a little increment. Calculated $G(r)$ by Shen (2007) utilizing the BJH method and the measured adsorption isotherm have the same features as above.

3.3 Hysteresis effect

It has been found that moisture content in the drying process is always higher than the corresponding wetting one, and the lag of water transport during dry procedure is called hysteresis effect. Many researchers have done a lot to explore this phenomenon and put forward different theories to explain the causes.

It can be explained by different curvature radii for wetting and drying processes. When wetting begins, pores can be referred to cylindrical shaped with two open ends (Fig. 1(b)), while drying goes with spherical meniscus (Fig. 1(a)). Different equilibrium humidity results from different n in Eq. (7). Neglect the adsorbed layer for simplification, equilibrium humidity in wetting process h_{ka} and drying process h_{kd} can be correlated as $h_{ka}^2 = h_{kd}$ under the same saturation degree Zhang *et al.* (2012).

It was also ever called as ink bottle effect Li (2009). Pores were assumed as a connection of cylindrical shaped with different radii. According to the Kelvin's equation, equilibrium humidity h_k for bigger pores is higher than that of smaller ones. During drying process, water can be stuck in bigger pores because of the failure of desorption for smaller pores, though the humidity decreases to the h_k of bigger pores. Parameter f_r was introduced by Maekawa *et al.* (2009) to explain the ink bottle effect. In their model, pores with radius smaller than the ones corresponding to the h_k is saturated during drying, while probabilities of condensation water exist for bigger ones, which can be expressed as

$$f_r = \begin{cases} 1 & , r \leq r_p \\ \int_0^{r_p} dV / \int_0^r dV & , r > r_p \end{cases} \quad (20)$$

Kondo *et al.* (2005) thought it was caused by different contact angles for wetting and drying processes Kondo *et al.* (2005). Some researchers held the opinion that the contact angle in wetting process is bigger than that in drying process, leading to the higher h_k in wetting process.

However, most researchers were inclined to the first two explanations in terms of cementitious materials. In this paper, both the first two explanations were taken into account. Computed

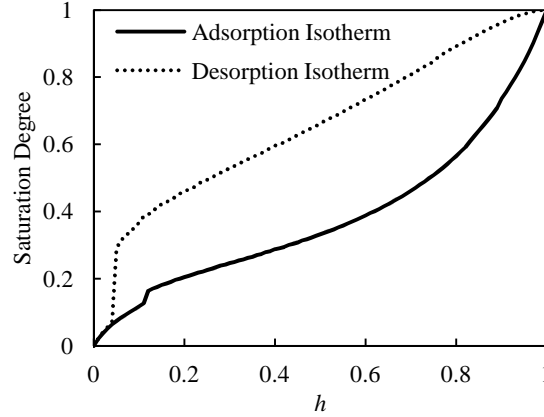


Fig. 5 Calculated adsorption / desorption isotherm for cement paste

adsorption isotherm and desorption isotherm were shown in Fig. 5 based on the curves of $w/c = 0.5$ in Fig. 4.

4. Moisture diffusivity based on pore-size distribution

Pores are the only access for moisture transport, so moisture diffusivity can be obtained starting with the transport equation in single pore. Assume that pores were instantly saturated after condensation. For pores with radius r , liquid flux in single pore J_l^r (kg/(m²•s)) can be described by Hagen-Poiseuille equation Welty *et al.* (2009)

$$J_l^r = -\rho_l \frac{r^2}{8\eta\tau} \text{grad}(p_c) = -\frac{r^2}{8\eta\tau} \frac{\rho_l^2 RT}{M_w h} \text{grad}(h) \quad (21)$$

where η is dynamic viscosity of liquid water, taking 0.9954×10^{-4} Pa•s for 20°C, and τ is tortuosity factor. For a uniformly random porous medium, $\tau = \pi^2/4$ Maekawa *et al.* (2009).

Different from vapor diffusion in air, vapor transport in pores is reduced by the molecular collisions against pore walls, which is called Knudsen effect. In this case vapor diffusivity in pores D_v (m²/s) should be modified as Daian (1988)

$$D_v = \frac{D_{va}}{1 + l_m / [2(r - t_a)]} \quad (22)$$

where D_{va} is vapor diffusivity in air, taking 2.17×10^{-5} m²/s for 20°C. According to the Fick's law, vapor flux in single pore J_v^r (kg/(m²•s)) under isotherm conditions is

$$J_v^r = -\frac{D_v}{\tau} \text{grad}(\rho_v) = -\frac{D_v}{\tau} \frac{p_{vs} M_w}{RT} \text{grad}(h) \quad (23)$$

Given that humidity is h and corresponding equilibrium radius is r_k for the pore with the actual radius r_p . The pores with the radius $r \leq r_p$ are fully saturated during the wetting process without

hysteresis effect, only liquid transport due to capillary condensation happens. While the other pores are still unsaturated with adsorbed layer. Because the force of pore walls is strong enough and the thickness of adsorbed layer is very thin, the adsorbed water can be assumed to be rigidly fixed on the pore wall Quenard and Sallee (1992), and only vapor diffusion exists in the pores with the radius bigger than r_p . Liquid diffusivity $D_{hcp,l}$ and vapor diffusivity $D_{hcp,v}$ for cement paste can be acquired by means of integration of the pore-size distribution.

Based on the Hagen-Poiseuille equation, liquid diffusivity was deduced by Maekawa *et al.* (2009), with consideration of the average flow behavior through a joint of pores of different radii. For cement paste, $D_{hcp,l}$ can be written as

$$D_{hcp,l} = \frac{1}{8} \left(\int_{r_{\min}}^{r_p} \frac{r-t_a}{\tau} \Phi G(r) dr \right)^2 \frac{\rho_l^2 RT}{\eta M_w h} \quad (24)$$

Take the integration from r_p to r_{\max} of D_v , vapor diffusivity of cement paste is generated as

$$D_{hcp,v} = \frac{p_{vs} M_w}{\tau RT} \int_{r_p}^{r_{\max}} \frac{\Phi D_{va}}{1 + l_m / [2(r-t_a)]} G(r) dr \quad (25)$$

For the drying process, pores $r > r_p$ may have condensation water because of the hysteresis effect. f_r (Eq. (20)) was introduced to represent the probability of hysteresis for each pore with $r > r_p$, with the assumption that the condensation water in the ink bottle is exclude out of the liquid transport. Then Eqs. (24) - (25) can be changed to

$$\begin{cases} D_{hcp,l} = \frac{1}{8} \left(\int_{r_{\min}}^{r_p} \frac{r-t_a}{\tau} f_r \Phi G(r) dr \right)^2 \frac{\rho_l^2 RT}{\eta M_w h} \\ D_{hcp,v} = \frac{p_{vs} M_w}{\tau RT} \int_{r_p}^{r_{\max}} \frac{(1-f_r) \Phi D_{va}}{1 + l_m / [2(r-t_a)]} G(r) dr \end{cases} \quad (26)$$

Whatever the wetting or drying process, percentages of pore volume taken up by vapor and liquid transport in cement paste can be unitedly expressed as

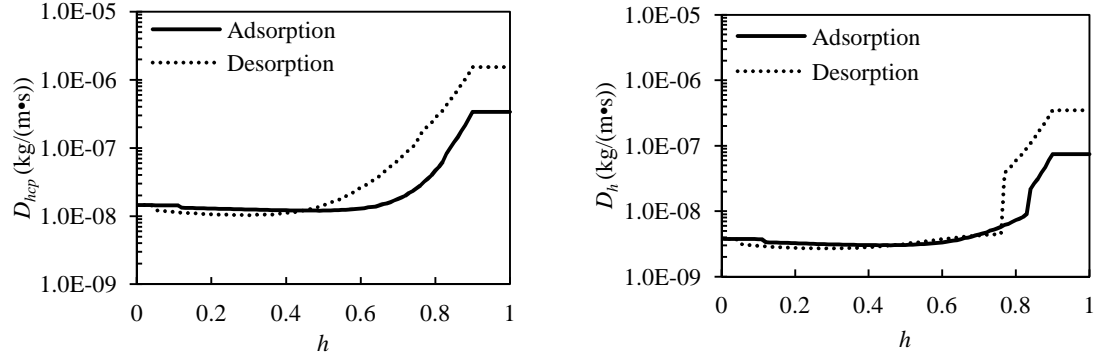
$$\begin{cases} g_l = \int_{r_{\min}}^{r_p} G(r) dr \\ g_v = \int_{r_p}^{r_{\max}} G(r) dr \end{cases} \quad (27)$$

Then the moisture diffusivity for cement paste is the combination of the vapor and liquid transport

$$D_{hcp} = D_{hl} g_l + D_{hv} g_v \quad (28)$$

As concrete can be regarded as a two-phase composite with cement paste and aggregate, moisture diffusivity of concrete could be evaluated using the composite theory, neglecting the influence of the interfacial transition zone Ababneh *et al.* (2003)

$$D_h = D_{hcp} \left(1 + \frac{g_{agg}}{g_{cp} / 3 + 1 / (D_{hagg} / D_{hcp} - 1)} \right) \quad (29)$$



(a) Calculated moisture diffusivity of cement paste (b) Calculated moisture diffusivity of concrete

Fig. 6 Calculated moisture diffusivity of cement paste and concrete

Where D_{hagg} and D_{hcp} are moisture diffusivity for aggregate and cement paste respectively, and g_{agg} and g_{cp} are volume fraction of aggregate and cement paste in concrete. Moisture diffusivity of aggregate can be assumed negligible compared with the cement paste for two reasons: (1) Porosity is small for materials such as granite, marble, quartzite and so on, which are commonly used as the aggregate in ordinary concrete Hall and Hoff (2012), Winkler (1994), Siegesmund (2011). (2) Pores in aggregates are discontinuous because of the scattered distribution of aggregate in concrete Ababneh *et al.* (2003).

Fig. 6 shows the calculated D_{hcp} and D_h for water cement ratio 0.5 using the $G(r)$ in Fig. 4. $\Phi_{cp}=36.5\%$ and $g_{agg}=0.65434$ were used. Neglecting the porosity of aggregate Φ_{agg} , porosity of concrete Φ_c was evaluated as $\Phi_{cp}/(1-g_{agg})$. It need to be noticed that, the hypothesis of capillary condensation happens in instant for pores with big radius would leading to the exaggerated increment of moisture diffusivity with the increasing of relative humidity h approaching to 1, though the exchange rate on the vapor-liquid interface is very large. So curves were flatted at the end starting from the point of $H_{flat}=0.9$ in Fig. 6 referring to the S-shaped curve proposed by Bažant and Najjar (1972).

It can be found from Fig. 6 that moisture diffusivity of concrete D_h is always lower than that of cement paste D_{hcp} , because of the lower moisture diffusivity of aggregate. Moisture diffusivities of both cement paste and concrete almost keep constant when the relative humidity is relatively low, and the vapor transport domains. When the relative humidity goes beyond 0.6-0.8, liquid transport will play an important role, leading to the sharp increase of diffusivities. Comparing the difference of moisture diffusivities during the process of water adsorption and desorption, it is also found that hysteresis effect generates the higher moisture content in desorption process and then higher diffusivities when the relative humidity is higher than 0.5 for cement paste or 0.8 for concrete.

5. Numerical simulation

5.1 Finite difference method

Specimen with the length of $2L$ was equally divided into $2m$ parts, and coordinate values for each point on the half side of the specimen starting from the exposed surface were $x_0, x_1, \dots, x_j, \dots$,

x_m respectively, setting the center of the specimens as the origin of coordinates. Transport time t was equally divided into n segments from the beginning of moisture transport, that is $t_0, t_1, t_2, \dots, t_m$. Implicit scheme of finite difference method, which was adapted in this paper for the stability of calculation results, was obtained by the discretization of Eq. (2) for one-dimensional transport and shown as follows

$$\rho_d \left(\frac{\partial W}{\partial h} \right)_j^k \bullet \frac{h_j^{k+1} - h_j^k}{t_{k+1} - t_k} = - \frac{\frac{D_{j+1}^k + D_j^k}{2} \bullet \frac{h_{j+1}^{k+1} - h_j^{k+1}}{x_{j+1} - x_j} - \frac{D_j^k + D_{j-1}^k}{2} \bullet \frac{h_j^{k+1} - h_{j-1}^{k+1}}{x_j - x_{j-1}}}{\frac{x_{j+1} + x_j}{2} - \frac{x_j + x_{j-1}}{2}} \quad (30)$$

When it comes to the symmetric one-dimensional transport, half of the total length, that is L , can be used in the calculation. Initial conditions for humidity are

$$h(x, 0) = h_0(x) \quad (31)$$

and the boundary conditions are

$$\begin{cases} h(0, t) = h_b(t) \\ (\partial h / \partial x)_{x=L} = 0 \end{cases} \quad (32)$$

Eq. (30) can be rewritten in the form of matrix with the combination of Eqs. (31) - (32)

$$\begin{bmatrix} b_1 & c_1 & & & & \\ a_2 & b_2 & c_2 & & & \\ & \ddots & \ddots & \ddots & & \\ & & a_j & b_j & c_j & \\ & & & \ddots & \ddots & \ddots \\ & & & & a_{m-1} & b_{m-1} & c_{m-1} \\ & & & & & a_m & b_m & c_m \end{bmatrix} \begin{Bmatrix} h_1^{k+1} \\ h_2^{k+1} \\ \vdots \\ h_j^{k+1} \\ \vdots \\ h_{m-1}^{k+1} \\ h_m^{k+1} \end{Bmatrix} = \begin{Bmatrix} f_1 - a_1 h_0^{k+1} \\ f_2 \\ \vdots \\ f_j \\ \vdots \\ f_{m-1} \\ f_m \end{Bmatrix} \quad (33)$$

where

$$\begin{cases} a_j = - \frac{D_j^k + D_{j-1}^k}{(x_j - x_{j-1})(x_{j+1} - x_{j-1})} \\ b_j = \frac{\rho_d (\partial W / \partial h)_j^k}{t_{k+1} - t_k} + \frac{D_{j+1}^k + D_j^k}{(x_{j+1} - x_j)(x_{j+1} - x_{j-1})} + \frac{D_j^k + D_{j-1}^k}{(x_j - x_{j-1})(x_{j+1} - x_{j-1})} \\ c_j = - \frac{D_{j+1}^k + D_j^k}{(x_{j+1} - x_j)(x_{j+1} - x_{j-1})} \\ f_j = \frac{\rho_d (\partial W / \partial h)_j^k}{t_{k+1} - t_k} h_j^k \end{cases} \quad (34)$$

Chasing method was used to solve Eq. (33). When the humidity distributions within cement paste or concrete for the previous time step were known as $(h_1^k, h_2^k, \dots, h_j^k, \dots, h_{m-1}^k, h_m^k)$, corresponding moisture diffusivities in the current time step $(D_1^k, D_2^k, \dots, D_j^k, \dots, D_{m-1}^k, D_m^k)$ can be obtained by the integration of pore-size distribution with diffusivities for the previous time step, and the humidity distributions for the current time step $(h_1^{k+1}, h_2^{k+1}, \dots, h_j^{k+1}, \dots, h_{m-1}^{k+1}, h_m^{k+1})$ would be figured out. Humidity on the surface was assigned as the environment ones, and the mean ambient temperature was used to simplify the analysis instead of the instant ones because of their little fluctuation.

Table 2 Mix proportion of concrete and cement paste specimens

Specimen	W: C: S: G	Water (kg/m ³)	Cement (kg/m ³)	Sand (kg/m ³)	Coarse aggregate (kg/m ³)
Concrete	0.5: 1 :1.45: 2.68	210	420	607	1127
Cement paste	0.5: 1	608	1216	/	/

5.2 Numerical results for cement paste and concrete specimens

Data in Guo's experiment Guo (2013) were used in this paper. Mix proportion of concrete and cement paste specimens was listed in Table 2. The specimens were 100 mm×150 mm×300 mm in size, cured at 23°C and 100%RH for 28 days. The internal relative humidity of a specimen was measured by small humidity sensors (DB170: Dalian Beifang M&C Engineering Co., Ltd., China) with 4 mm width and 2 mm thickness embedded. The 4 non-exposed surfaces were sealed by epoxy to ensure the symmetric one-dimensional transport. After then the specimens with humidity sensors inside were settled in the environment chamber, which was set to be different humidity and temperatures to simulate the wetting and drying processes.

Due to space limitations of this paper, only a part of typical measured humidity response in cement paste and concrete are shown in Figs. 7-10. They are measured in wetting process with boundary conditions of 20°C, 100%RH lasting for 57days for cement paste specimens and 20°C, 100%RH lasting for 59 days for concrete specimens, while in drying process 20°C, 17%RH lasting for 28 days for cement paste specimens and 55°C, 3%RH lasting for 28 days for concrete specimens. Simulated relative humidity response at different locations from the exposed surface under wetting condition and drying condition for concrete with $w/c = 0.5$ were compared with measured results in Figs. 7-8 respectively. Mark MIP in the two figures represents that the curves were calculated with the pore-size distribution measured by mercury intrusion porosimetry in Guo's experiments, while CI means that the calculated pore-size distribution in Fig. 4 was used. Set $\rho_{cpd} = 1637 \text{ kg/m}^3$, which was the mean value of the measured results in the experiment for cement paste specimens with $w/c=0.5$. Values of other parameters were the same as above.

Simulated relative humidity response at different locations from the exposed surface under wetting condition and drying condition for concrete with $w/c = 0.5$ were compared with measured results in Figs. 9-10 respectively. Meanings of mark MIP and CI in the two figures were the same as Figs. 7-8. Set apparent density for dry concrete $\rho_{cd} = 2572 \text{ kg/m}^3$, which was the mean value of the measured results in the experiment for concrete specimens with $w/c = 0.5$. Values of other parameters were the same as above.

It can be seen from Figs. 7-10 that, whatever the pore-size distribution is obtained by measured MIP or calculated CI, predictions of the inner humidity well capture the trend of the moisture humidity of measured ones.

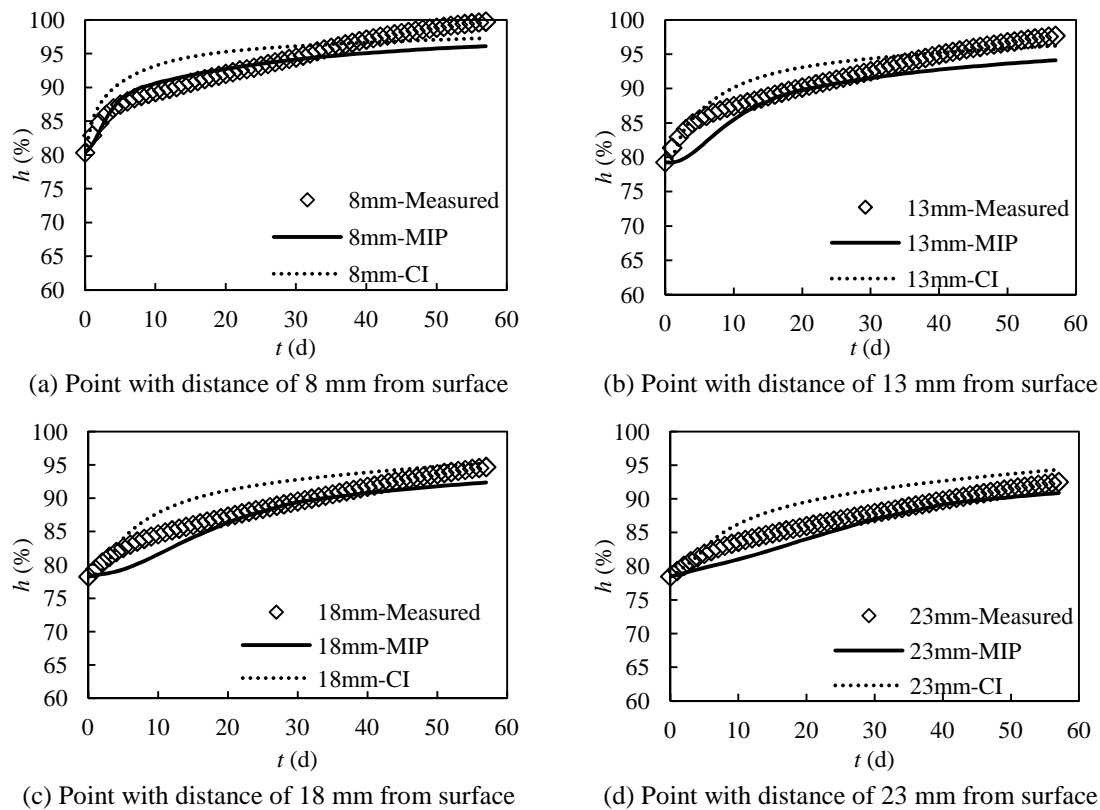


Fig. 7 Comparison between simulated and measured relative humidity under wetting condition for cement paste

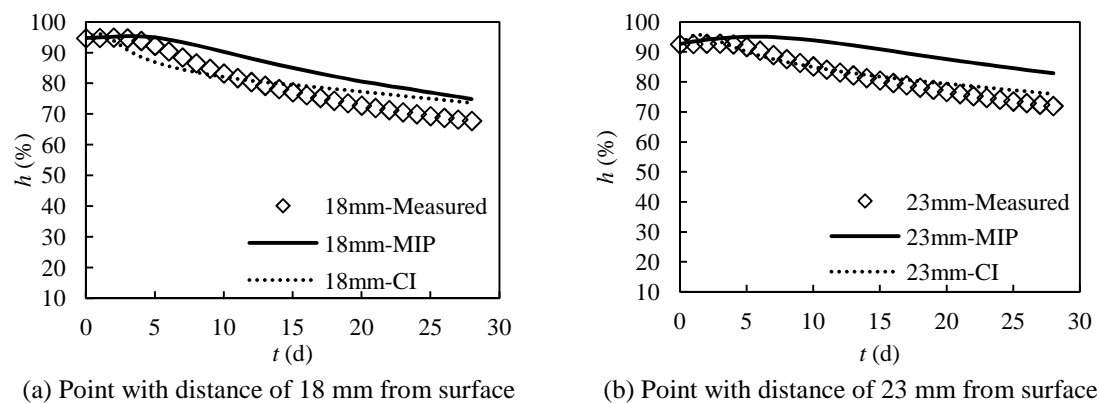
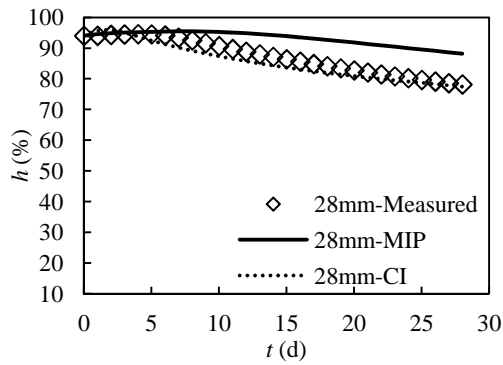
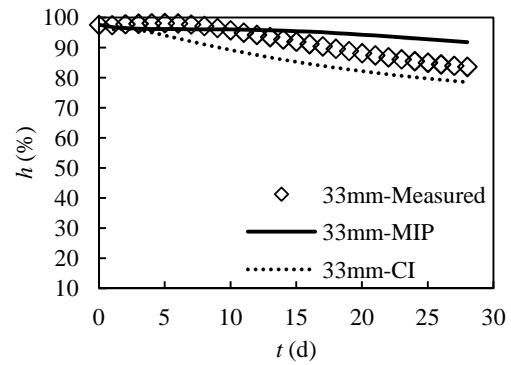


Fig. 8 Comparison between simulated and measured relative humidity under drying condition for cement paste

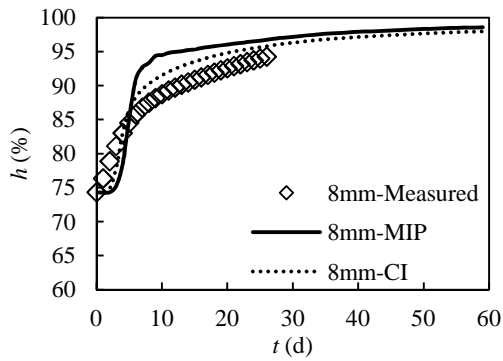


(c) Point with distance of 28mm from surface

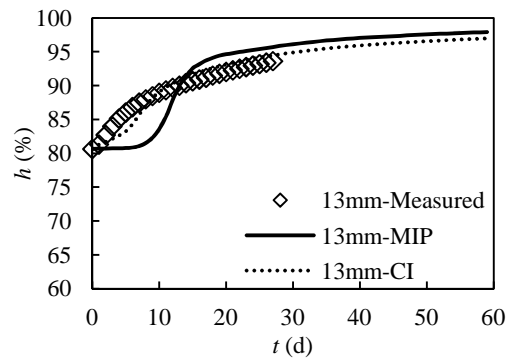


(d) Point with distance of 33mm from surface

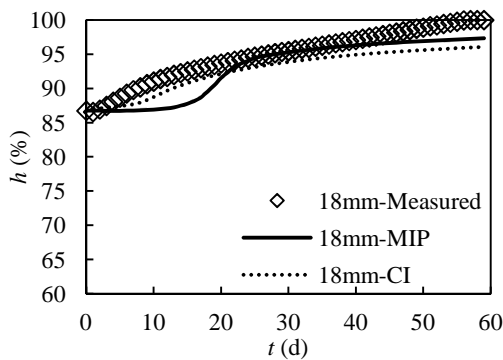
Fig. 8 Continued



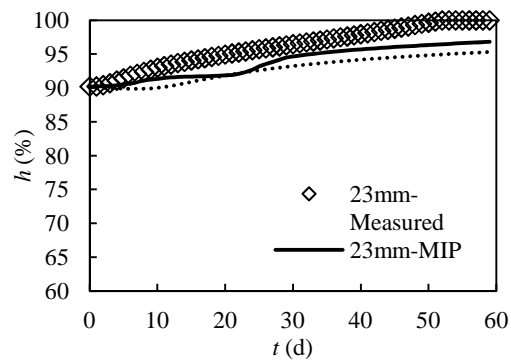
(a) Point with distance of 8 mm from surface



(b) Point with distance of 13 mm from surface



(c) Point with distance of 18 mm from surface



(d) Point with distance of 23 mm from surface

Fig. 9 Comparison between simulated and measured relative humidity under wetting condition for concrete

However, small difference between the calculated humidity response and measured ones for concrete can be observed due to the neglecting of the influence of interfacial transition zone (ITZ) between cement paste and aggregate in concrete. It is well known that the deficiency of the porosity of ITZ leads to a smaller calculated porosity of concrete, and then a smaller moisture

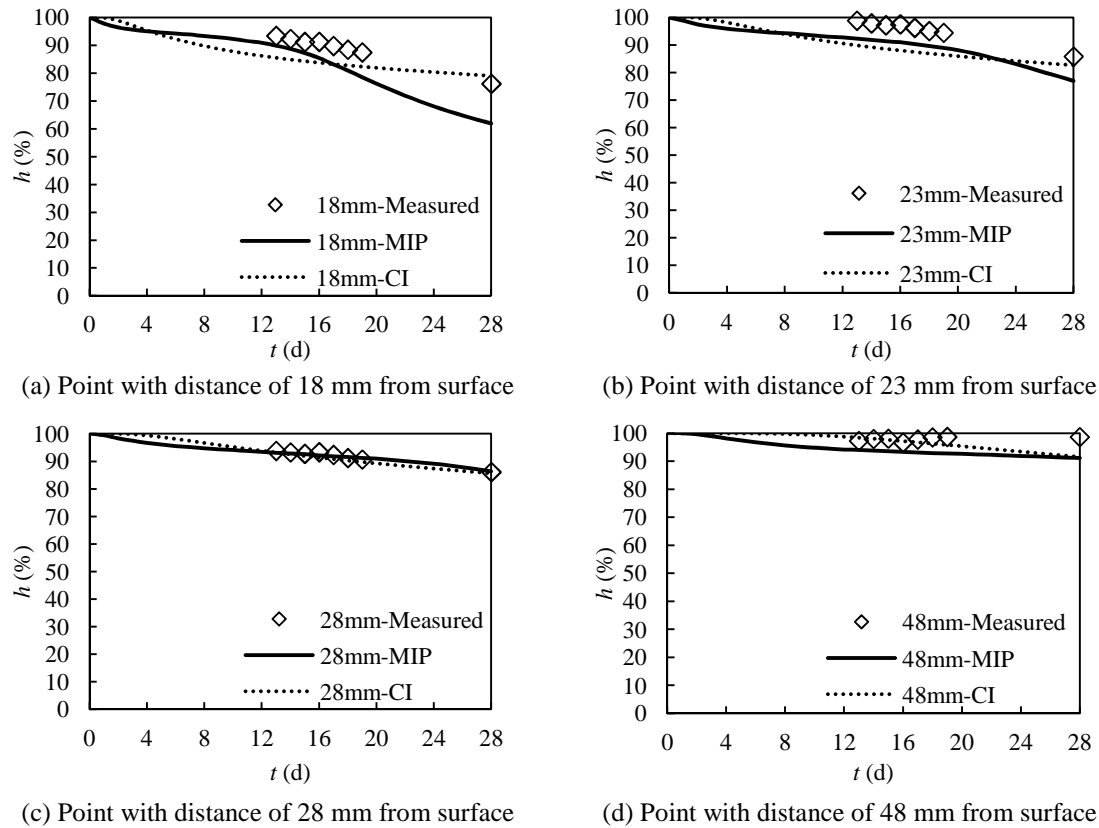


Fig. 10 Comparison between simulated and measured relative humidity under drying condition for concrete

diffusivity. So for the concrete under wetting condition in Fig. 9, moisture transports from the surface into the inner concrete, the calculated moisture response at the deeper location from the surface was smaller than the measured ones.

For the concrete under drying condition in Fig. 9, moisture transports from the inner concrete to the surface, the calculated moisture response at the closer location to the surface was smaller than the measured ones. As drying or wetting process last longer, major difference might be expected.

6. Conclusions

- Moisture transport in concrete in atmospheric environment was studied in this paper. A simplified formula for the thickness of the adsorbed layer was proposed utilizing the Kelvin's equation and Hillerborg's equation, simplifying the calculation procedure. Based on the basic idea of BJH method, the pore-size distribution functions of cement paste with different water cement ratios were calculated with the water adsorption isotherms, which combined the water cement ratios with the pore-size distributions of cement paste in a theoretical way.

- Taking into consideration of hysteresis effect, the moisture diffusivity of cement paste in wetting and drying process was obtained by the integration of calculated pore-size distribution.

Composite theory was utilized here to give the prediction of moisture diffusivity of concrete, neglecting the moisture diffusivity of aggregate. The calculated moisture diffusivity shows the changing influence of vapor and liquid transport in the whole humidity range.

- MIP or CI data were used in the numerical analysis of humidity response, and the ITZ was simply discussed. Simulation results shows that the numerical analysis well capture the trend of the measured values, which proves that the calculation procedure can be used to predict the humidity distribution in practice.

Acknowledgements

The research described in this paper was financially supported by the National High Technology Research and Development Program of China (863 Program, No. 2012AA050903).

References

- Ababneh, A., Benboudjema, F. and Xi, Y.P. (2003), "Chloride penetration in nonsaturated concrete", *J. Mater. Civ. Eng.*, **15**(2), 183-191.
- Barrett, E.P., Joyner, L.G. and Halenda, P.P. (1951), "The determination of pore volume and area distributions in porous substances. I. computations from nitrogen isotherms", *J. Am. Chem. Soc.*, **73**(1), 373-380.
- Bažant, Z.P. and Najjar, L.J. (1972), "Nonlinear water diffusion in nonsaturated concrete", *Mater. Struct.*, **5**(1), 3-20.
- Brunauer, S., Emmett, P.H. and Teller, E. (1938), "Adsorption of gases in multimolecular layers", *J. Am. Chem. Soc.*, **60**(2), 309-319.
- Brunauer, S., Skalny, J. and Bodor, E.E. (1969), "Adsorption on nonporous solids", *J. Colloid Interface Sci.*, **30**(4), 546-552.
- Cranston, R.W. and Inkley, F.A. (1957), "The determination of pore structures from nitrogen adsorption isotherms", *Advan. Catal.*, **9**, 143-154.
- Daian, J.F. (1988), "Condensation and isothermal water transfer in cement mortar, part I - pore size distribution, equilibrium water condensation and imbibition", *Trans. Porous Media*, **3**(6), 563-589.
- Daian, J.F. (1989), "Condensation and isothermal water transfer in cement mortar, part II - transient condensation of water vapor", *Trans. Porous Media*, **4**(1), 1-16.
- Eskandari-Ghadi, M., Zhang, W.P., Xi, Y.P. and Stein, S. (2013), "Modeling of moisture diffusivity of concrete at low temperatures", *J. Eng. Mech.*, **139**(7), 903-915.
- Garrabrants, A.C. and Kosson, D.S. (2003), "Modeling moisture transport from a Portland cement-based material during storage in reactive and inert atmospheres", *Dry. Technol.*, **21**(5), 775-805.
- Gawin, D., Majorana, C.E. and Schrefler, B.A. (1999), "Numerical analysis of hygro-thermal behavior and damage of concrete at high temperature", *Mech. Cohes.-Frict.Mater.*, **4**(1), 37-74.
- Guo, B.H. (2013), "Carbonation model of concrete considering coupling transfer of heat and moisture", Master Dissertation, Tongji University, Shanghai. (in Chinese)
- Hall, C. and Hoff, W.D. (2012), *Water transport in brick, stone and concrete*, 2nd Edition, CRC Press, Boca Raton, FL., USA.
- Hillerborg, A. (1985), "A modified absorption theory", *Cement Concrete Res.*, **15**(5), 809-816.
- Ishida, T., Maekawa, K. and Kishi, T. (2007), "Enhanced modeling of moisture equilibrium and transport in cementitious materials under arbitrary temperature and relative humidity history", *Cement Concrete Res.*, **37**(4), 565-578.
- Kondo, S., Ishikawa, T. and Abe, I. (2005), *Adsorption science*, 2nd Edition, Translated by Li, G.X.,

- Chemical Industry Press, Beijing. (in Chinese)
- Leech, C., Lockington, D. and Dux, P. (2003), "Unsaturated diffusivity functions for concrete derived from NMR images", *Mater. Struct.*, **36**(6), 413-418.
- Li, C.Q. and Li, K.F. (2010), "Moisture transport in concrete cover under drying-wetting cycles: theory, experiment and modeling", *J. Chin. Ceram. Soc.*, **38**(7), 1151-1159. (in Chinese)
- Li, C.Q. (2009), "Study on water and ionic transport processes in cover concrete under drying-wetting cycles", Ph.D. Dissertation, Tsinghua University, Beijing. (in Chinese)
- Maekawa, K., Ishida, T. and Kishi, T. (2009), *Multi-scale modeling of structural concrete*, Taylor & Francis, London and New York.
- Quenard, D. and Sallee, H. (1992), "Water vapour adsorption and transfer in cement-based materials: a network simulation", *Mater. Struct.*, **25**(9), 515-522.
- Rose, D.A. (1963), "Water movement in porous materials: part 2 - the separation of the components of water movement", *Brit. J. Appl. Phys.*, **14**(8), 491-496.
- Sakata, K. (1983), "A study on moisture diffusion in drying and drying shrinkage of concrete", *Cem. Concr. Res.*, **13**(2), 216-224.
- Shen, C.H. (2007), "Researches on the moisture transport of cement-based materials", Ph.D. Dissertation, Wuhan University of Technology, Wuhan. (in Chinese)
- Siegesmund, S. (2011), *Stone in architecture: properties, durability*, 4th Edition, Springer-Verlag Berlin Heidelberg, Berlin, Germany.
- Ramachandran, V.S. and Feldman, R.F. (1984), *Concrete admixture handbook-properties, science, and technology*, 2nd Edition, Noyes Publication, Park Ridge, NJ, USA.
- Welty, J.R., Wicks, C.E., Wilson, R.E. and Rorrer, G.L. (2009), *Fundamentals of momentum, heat, and mass transfer*, 5th Edition, John Wiley & Sons, Inc, Hoboken, NJ, USA.
- Winkler, E.M. (1994), *Stone in architecture: properties, durability*, Springer-Verlag, Berlin, Germany.
- Xi, Y.P., Bažant, Z.P. and Jennings, H.M. (1994a), "Moisture diffusion in cementitious materials moisture capacity and diffusivity", *Adv. Cem. Based Mater.*, **1**(6), 258-266.
- Xi, Y.P., Bažant, Z.P. and Jennings, H.M. (1994b), "Moisture diffusion in cementitious materials moisture adsorption isotherms", *Adv. Cem. Based Mater.*, **1**(6), 248-257.
- Zhang, Q.Z. (2012), "Study on similarity of accelerated corrosion tests for concrete in tidal zone", Ph.D. Dissertation, Tongji University, Shanghai. (in Chinese)
- Zhang, Q.Z., Gu, X.L., Zhang, W.P. and Huang, Q.H. (2012), "Model on capillary pressure-saturation relationship for concrete", *J. Tongji Univ.: Nat. Sci. Ed.*, **40**(12), 1753-1759. (in Chinese)